Rate equation description of quantum noise in nanolasers with few emitters

Mørk, Jesper; Lippi, G. L.

Published in:
Applied Physics Letters

Link to article, DOI:
10.1063/1.5022958

Publication date:
2018

Document Version
Publisher's PDF, also known as Version of record

Rate equation description of quantum noise in nanolasers with few emitters

J. Mork, and G. L. Lippi

Citation: Appl. Phys. Lett. **112**, 141103 (2018); doi: 10.1063/1.5022958
View online: https://doi.org/10.1063/1.5022958
View Table of Contents: http://aip.scitation.org/toc/apl/112/14
Published by the American Institute of Physics

Rate equation description of quantum noise in nanolasers with few emitters

J. Mork[1,a)] and G. L. Lippi[2]
[1]*DTU Fotonik, Technical University of Denmark, 2800 Kongens Lyngby, Denmark*
[2]*Université Côte Azur, Institut de Physique de Nice, UMR 7010 CNRS, Nice, France*

(Received 19 January 2018; accepted 22 March 2018; published online 2 April 2018)

Rate equations for micro- and nanocavity lasers are formulated which take account of the finite number of emitters, Purcell effects as well as stochastic effects of spontaneous emission quantum noise. Analytical results are derived for the intensity noise and intensity correlation properties, $g^{(2)}$, using a Langevin approach and are compared with simulations using a stochastic approach avoiding the mean-field approximation of the rate equations. Good agreement between the two approaches is found even for large values of the spontaneous emission beta-factor, i.e., for threshold-less lasers, as long as more than about ten emitters contribute to lasing. A large value of the beta-factor improves the noise properties. https://doi.org/10.1063/1.5022958

The spontaneous emission β-factor, i.e., the ratio between the spontaneous emission rate into the dominant lasing mode and the total emitter decay rate, plays an important role in the transition to lasing and quantum noise.[1–3] It was thus shown that β characterizes the system size, and in the thermodynamic limit of $\beta^{-1} \to \infty$, the concept of laser threshold is well-defined, while for $\beta \to 1$, the laser operates in the cavity-QED limit of thresholdless lasing.[2] Standard edge emitting and surface emitting lasers have $\beta \simeq 10^{-5}$–10^{-4}, i.e., operate in the thermodynamic limit, and their properties are well understood.[4] Recent experiments have demonstrated high-β lasers using ultra-small photonic crystal cavities,[5–8] micropillar structures,[9,10] and metal-clad cavities,[11] prompting the question of the noise properties of these lasers.

In this paper, we generalize the standard semiconductor laser rate equations[4] to cover the case of ultra-small and high-β lasers containing only a few discrete emitters. Analytical expressions for the steady-state intensity noise and second-order intensity correlation, $g^{(2)}(0)$, are derived using a small-signal Langevin approach and compared with stochastic simulations taking into account the discrete nature of photons and electrons. Very good agreement between the two approaches is found in general, with small deviations occurring around threshold when less than 10 emitters contribute to lasing.

While several models are already available for microcavity and nanocavity lasers, see e.g. Refs. 1 and 12–20, these differ on a number of issues, e.g. how to incorporate the spontaneous emission factor and Purcell enhancement. As we shall discuss, one cannot in general apply a Purcell enhancement factor to the stimulated emission rate. A recent theoretical study[17] found that high-β lasers have a much higher noise level than that expected from standard rate equations, an effect attributed to discrete birth-death processes initiating additional dynamics, which becomes important for a moderate number of emitters and photons. In contrast, we find near-perfect agreement between our nanolaser rate equation model and discrete stochastic simulations.

Figure 1 shows a schematic defining important variables describing the nanocavity laser, i.e., number n_0 of emitters (dipoles), number n_p of photons in the cavity mode, decay rate γ_c of the cavity population, and the coupling rate γ_r between photons in the cavity mode and a single emitter. If the polarization of the medium decays on a timescale that is short compared to the other characteristic time constants of the laser, due to various dephasing processes, the polarization can be eliminated adiabatically. These de-coherence processes also allow one to neglect quantum mechanical correlations,[16] and the laser dynamics can be described as rate equations for the (classical) photon and carrier number

$$\frac{dn_e}{dt} = P_{pu} - R_{st} - R_{sp} - R_{bg} + F_e(t), \tag{1}$$

$$\frac{dn_p}{dt} = R_{st} + R_{sp} - R_c + F_p(t). \tag{2}$$

Here, P_{pu} is the pump rate into the upper laser level, taking into account Pauli blocking,[16] R_{st} and R_{sp} are the net rates of stimulated and spontaneous emission into the cavity mode, R_{bg} is the (background) rate of spontaneous emission into all modes, but the cavity mode, as well as non-radiative emission, and R_c is the photon escape rate from the cavity. Furthermore, $F_n(t)$ and $F_p(t)$ are stochastic Langevin forces. The open nature of the cavity may be given firm ground by the use of a quasi-bound state basis, allowing consideration of complex cavities.[21,22]

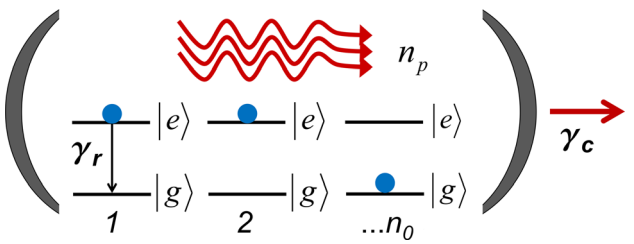

FIG. 1. Illustration of emitters embedded in a cavity and interacting with photons in the cavity mode.

a)Electronic mail: jesm@fotonik.dtu.dk

Denoting by n_e the number of emitters in the excited state and assuming charge neutrality (for quantum dot lasers, the lower level is in the valence band and the upper is in the conduction band), the number of emitters in the ground state is $n_g = n_0 - n_e$. The rates entering (1) and (2) then become: $P_{pu} = \gamma_p(n_0 - n_e)$, $R_{sp} = \gamma_r n_e$, $R_{bg} = \gamma_{bg} n_e$, $R_c = \gamma_c n_p$, and $R_{st} = R_{eg} - R_{ge}$ with $R_{eg} = \gamma_r n_e n_p$, $R_{ge} = \gamma_r(n_0 - n_e)n_p$, and (1) and (2) read

$$\frac{dn_e}{dt} = \gamma_p(n_0 - n_e) - \gamma_r(2n_e - n_0)n_p - \gamma_t n_e + F_e, \quad (3)$$

$$\frac{dn_p}{dt} = \gamma_r(2n_e - n_0)n_p + \gamma_r n_e - \gamma_c n_p + F_p. \quad (4)$$

The β-factor enters the rate equations via the ratio

$$\beta = \frac{\gamma_r n_e}{\gamma_t n_e} = \frac{\gamma_r}{\gamma_t} = \frac{\gamma_r}{\gamma_r + \gamma_{bg}}, \quad (5)$$

with $\gamma_t = \gamma_r + \gamma_{bg}$ being the total decay rate and γ_{bg} being the background rate into other modes. For inhomogeneously broadened systems, such as quantum dots with more levels and wetting layer transitions, β will in general depend on the total carrier density.[15,20] Notice that the pump-blocking term $\gamma_p(n_0 - n_e)$ ensures that only a finite number of emitters (n_0) are considered.

If spontaneous emission into the lasing mode is neglected, the threshold value for the pump rate per emitter, beyond which the photon number acquires a positive value, and the (clamped) number of emitters become

$$\gamma_{pu,th} = \frac{n_0\gamma_r + \gamma_c}{n_0\gamma_r - \gamma_c}\gamma_t, \quad n_{e,th} = \frac{1}{2}n_0 + \frac{1}{2}\frac{\gamma_c}{\gamma_r}, \quad (6)$$

showing that lasing is only possible for $n_0\gamma_r > \gamma_c$, i.e., when the maximum gain exceeds the cavity losses.[4] The corresponding rate of outcoupled photons becomes $\gamma_c n_p = (\gamma_p - \gamma_{pu,th})(n_0 - \gamma_c/\gamma_r)/2$.

In general, the coupling rate of a single emitter with dipole moment d to the quasi-mode of a cavity is in the weak-coupling limit[16,23,24]

$$\gamma_r = \frac{2d^2}{\hbar\epsilon_0 n^2 V_p}\frac{\omega_0}{\gamma_c + 2\gamma_2}. \quad (7)$$

We have assumed the emitter transition frequency, ω_0, to coincide with the mode resonance and the emitter to be placed in an antinode of the cavity field, aligned with the field polarization. Further, V_p is the *modal* volume, n the refractive index, and γ_2 the total emitter dephasing rate. Phonon-assisted[24] and Auger transitions[25] are neglected. The Purcell factor corresponding to Eq. (7) is $F_p = \gamma_r/\gamma_{r,hom} = 3/(4\pi^2 V_p)(\lambda/n)^3\omega_0/(\gamma_c + 2\gamma_2)$, where $\gamma_{r,hom} = d^2\omega_0^3 n/(3\pi\epsilon_0\hbar c^3)$ is the emission rate of the same emitter in a homogeneous material with index n. Figure 2 shows the variation of γ_r and β with the cavity Q-factor, $Q = \omega_0/\gamma_c$, for different dephasing times, $T_2 = 1/\gamma_2$.

For $\gamma_c \gg \gamma_2$, we find the usual expression[26,27] for the Purcell factor, $F_p \propto Q$. The expression (7) is more general, also accounting for emitter broadening.[23,24] It shows that with increasing γ_c or γ_2, the radiative rate is lowered, reflecting in both cases that the effective interaction time between the cavity excitation and the emitter is reduced. As mentioned earlier, the rate equations require $\gamma_2 \gg \gamma_c$ and γ_t to be valid, excluding their use for the analysis of "bad-cavity" effects[28] and collective phenomena.[29] This implies that expression (7) for γ_r has to be evaluated in the limit $\gamma_c = 0$, corresponding to infinite Q, when used for rate Eqs. (3) and (4). This agrees with conventional procedures for calculating the gain coefficient of semiconductor lasers.[4] Here, one calculates the net stimulated rate for a given photon density in the considered *single mode*, and the corresponding spontaneous emission rate into that mode is the stimulated rate with one photon in the mode. This takes into account emitter broadening, but not cavity broadening, the addition of which will only act to decrease the radiative rate. The presence of Purcell enhancement, $F_p > 1$, therefore cannot be taken as indication that the stimulated emission rate (gain) of the laser has increased beyond the value obtained in the absence of Purcell effects.

The inverse dependence on the photon volume of γ_r, Eq. (7), also implies an enhancement effect for small volumes. Notice that this effect is also included in standard semiconductor laser theories,[4] where it often is implicit by working with photon and carrier *densities* and introducing the confinement factor, $\Gamma = V_e/V_p$, where V_e is the volume of active material. By comparing with standard rate equations, we find the correspondence

$$2\gamma_r \to \frac{v_g g_N}{V_p} = \frac{\Gamma v_g g_N}{V_e}, \quad (8)$$

where g_N is the differential gain and v_g is the group velocity. The factor of two in this expression arises because the transparency carrier density introduced in standard gain models corresponds to $0.5n_0/V_e$.

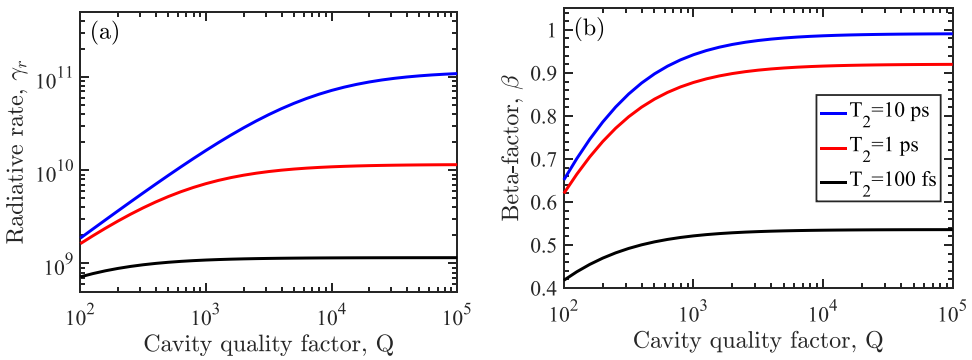

FIG. 2. Variation of (a) γ_r and (b) β with the cavity Q-factor for different values of the dephasing time. $\lambda = 2\pi c/\omega_0 = 1.55\,\mu$m, $n = 3.3$, $d = 1 \times 10^{-28}$ Cm, $V_p = (\lambda/n)^3$, and $\gamma_{bg} = 1 \times 10^9\,\mathrm{s}^{-1}$.

In laser cavities realized using photonic crystals, e.g. line-defect cavities,[5,7,30,31] the group velocity is reduced due to strong dispersion. It has been shown that slow light effects give rise to an enhancement of the gain per unit length.[32,33] However, the *temporal* gain coefficient entering laser rate equations for cavity quantities, such as the total photon number, is unaffected since the laser roundtrip time is also increased in proportion to the group refractive index.[31] The group velocity entering (8) is thus the background value not taking into account the longitudinal perturbation of the refractive index.[31,34]

We now perform a small-signal analysis of rate Eqs. (3) and (4) with Langevin noise terms that have the usual correlation properties, $\langle F_x(t_1)F_y(t_2)\rangle = 2D_{xy}\delta(t_1-t_2)$. The diffusion coefficients D_{xy} are obtained using the McCumber approach, see Ref. 4, $2D_{pp} = \gamma_c\bar{n}_p + \gamma_r\bar{n}_e + \gamma_r n_0\bar{n}_p$, $2D_{pe} = 2D_{ep} = -\gamma_r n_0\bar{n}_p - \gamma_r\bar{n}_e$, and $2D_{ee} = \gamma_p(n_0-\bar{n}_e) + \gamma_t\bar{n}_e + \gamma_r n_0\bar{n}_p$. By integrating the spectrum of the photon number fluctuations over all frequencies, we get the following simple expression for the variance of the photon number:

$$\langle \Delta n_p^2\rangle = \frac{1}{\Gamma}\left[\left(1+\frac{\Gamma_{ee}^2}{\omega_R^2}\right)D_{pp} + \frac{\Gamma_{pe}^2}{\omega_R^2}D_{ee} + \frac{2\Gamma_{pe}\Gamma_{ee}}{\omega_R^2}D_{pe}\right], \quad (9)$$

where $\langle \Delta n_p^2\rangle \equiv \langle (n_p - \langle n_p\rangle)^2\rangle = \langle n_p^2\rangle - \langle n_p\rangle^2$. We defined the following quantities: $\Gamma_{ee} = \gamma_p + \gamma_t + 2\gamma_r\bar{n}_p$, $\Gamma_{ep} = \gamma_r(2\bar{n}_e - n_0)$, $\Gamma_{pe} = \gamma_r(2\bar{n}_p + 1)$, $\Gamma_{pp} = \gamma_c - \gamma_r(2\bar{n}_e - n_0)$, $\omega_R^2 \equiv \Gamma_{ee}\Gamma_{pp} + \Gamma_{pe}\Gamma_{ep}$, and $\Gamma = \Gamma_{ee} + \Gamma_{pp}$. If the lower level population is neglected and one assumes $n_p \gg 1$, this result reduces to that derived in Ref. 35.

Using (9), we obtain analytical expressions for the relative intensity noise, RIN, the Fano factor,[2] F_F, and the second-order intensity correlation

$$\mathrm{RIN} = \frac{\langle \Delta n_p^2\rangle}{\langle n_p\rangle^2}, \quad F_F = \frac{\langle \Delta n_p^2\rangle}{\langle n_p\rangle}, \quad g^{(2)}(0) = \frac{\langle n_p(n_p-1)\rangle}{\langle n_p\rangle^2}. \quad (10)$$

Notice that for a Poisson process, the variance equals the mean, $\langle \Delta n_p^2\rangle = \langle n_p\rangle$, and we have $F_F = 1$, $g^{(2)}(0) = 1$, and $RIN = 1/\langle n_p\rangle$.

For nanolasers with a small photon number, it is not obvious that a small-signal analysis correctly describes the noise properties. Close to laser threshold and below, spontaneous emission of a single photon may thus constitute a large perturbation of the state of the laser, which is not well described by linearized equations. Furthermore, for high-β lasers, the threshold regime extends over a large range of pump rates. In order to establish the accuracy of the analytical results, we compare these with simulations without the assumptions of the Langevin analysis.

We follow ideas[36] for describing the laser dynamics as a stochastic process of discrete events representing the various recombination and photon generation mechanisms but extend these results to include a finite number of emitters. For a chosen time increment, Δt, the time evolution of $n_p(t)$ is described by a discrete stochastic process, i.e., $n_p(i\Delta t) \to n_{p,i}$, and similarly for n_e. Thus, $n_{p,i+1} = n_{p,i} + \Delta n_{cv} - \Delta n_{vc} + \Delta n_{sp} - \Delta n_c$, where Δn_x are sequences of integer, non-negative random numbers with probability distributions that lead to the same average rates as expressed by the rates in (3) and (4) and obeying the statistics of the underlying processes. For example, the probability of obtaining the outcome $\Delta n_c = m$ corresponds to the probability of getting m occurrences, with n_p draws, each of which having a success probability of $\gamma_c\Delta t$: $\Delta n_c \sim \mathcal{P}(n_p, \gamma_c\Delta t)$. We shall here assume a sufficiently short time increment, Δt, that the probability distribution $\mathcal{P}$ is given by a Poisson process, i.e., $\mathcal{P}(n_p, \gamma_c\Delta t) \simeq \mathcal{P}_P(n_p\gamma_c\Delta t)$, with both the mean value and the variance given by $\lambda = n_p\gamma_c\Delta t$. Figure 3 compares stochastic simulations (markers) and analytical results (solid lines) for the cavity photon number, the RIN, and the second-order intensity correlation $g^{(2)}(0)$. The pump rate used here is the total rate, taken as $\gamma_p n_0$, considering that pumping of the emitters effectively proceeds via levels below and above the laser ground and excited states, respectively. The total emitter decay rate and the cavity decay rate are fixed, and the results are shown for three different pairs of values for the spontaneous emission factor and the number of emitters, i.e., $\beta = 0.001$, $n_0 = 20000$ (blue), $\beta = 0.1$, $n_0 = 200$ (red), and $\beta = 1$, $n_0 = 20$ (black). Notice that for a constant value of the total decay rate of excited emitters, γ_t, the radiative rate γ_r scales with β and a larger number of emitters are therefore required to reach lasing as β is reduced, also see (6).

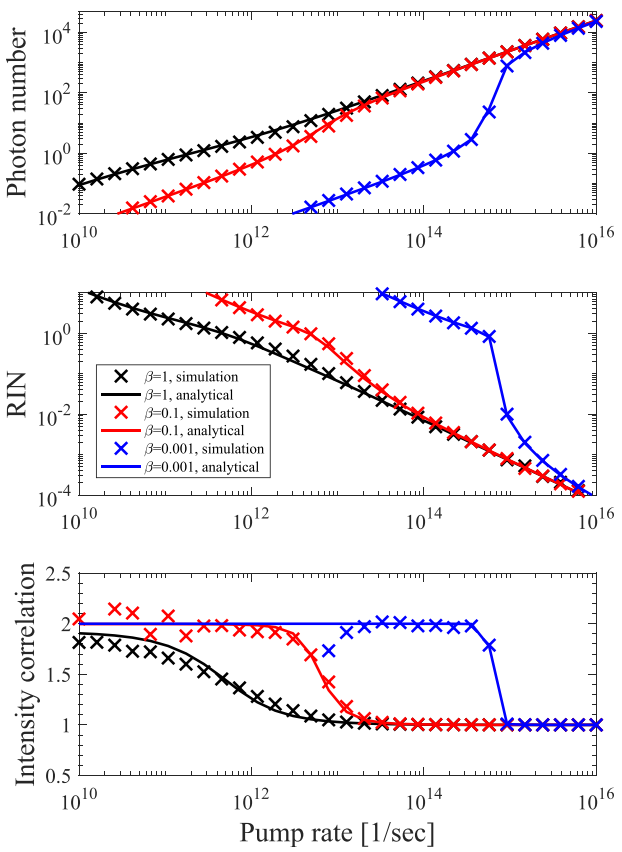

FIG. 3. Analytical (solid lines) and simulated (markers) results for the variation of output power (upper panel), RIN (middle), and intensity correlation, $g^{(2)}(0)$, (lower) with pump rate, $\gamma_p n_0$, for different values of the spontaneous emission factor: $\beta = 0.001$ (blue), 0.1 (red), and 1 (black). The total emitter decay rate, $\gamma_t = 1\times10^{10}\,\mathrm{s}^{-1}$, and cavity decay rate, $\gamma_c = 1\times10^{11}\,\mathrm{s}^{-1}$, are fixed. For $\beta = 0.001$, simulations for low pump rates are discarded due to statistical uncertainty.

For the photon number and RIN, very good agreement between the analytical results and the simulations is obtained, with minor deviations occurring around laser threshold. The intensity correlation shows the expected change from thermal statistics, $g^{(2)}(0)=2$, below threshold to Poissonian statistics, $g^{(2)}(0)=1$, above threshold.[10,37] For $\beta=0.1$ and 0.001, jumps are seen in the photon number close to threshold, while $\beta=1$ shows the apparent thresholdless characteristic.[2] Recently, super-thermal statistics, $g^{(2)}(0)>2$, was obtained below threshold and associated with the occurrence of collective effects among the emitters,[38] which are neglected in our model. This was shown to be a good approximation when the cavity decay rate is much smaller than the emitter dephasing rate.[29] We notice that for pump rates well below threshold, very long simulations are required to get statistically significant results for $g^{(2)}(0)$. However, except for $\beta=1$ and around threshold, excellent agreement between simulations and analytical results is obtained. A conclusion to be drawn from Fig. 3 is that increasing β is advantageous for reducing the intensity noise. This is perhaps not surprising, given that γ_r scales with β for a constant total decay rate, γ_t.

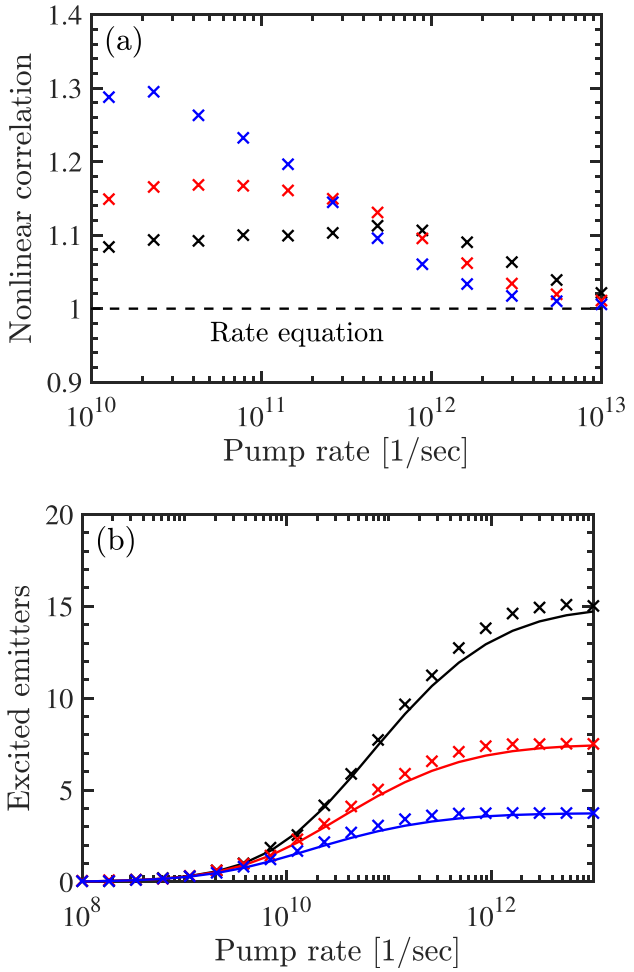

FIG. 4. Accuracy of mean-field approximation. (a) The ratio $\langle n_p n_e\rangle/(\langle n_p\rangle\langle n_e\rangle)$ is shown versus pump rate for different numbers of emitters, $n_0=5$ (blue), $n_0=10$ (red), and $n_0=20$ (black). The cavity decay rate is varied in order to keep the threshold pump rate per emitter fixed, i.e., $\gamma_c/n_0=5\times10^9\,\mathrm{s}^{-1}$, while $\beta=1$ and $\gamma_t=1\times10^{10}\,\mathrm{s}^{-1}$ are constant. (b) Excited number of emitters; solid lines are rate-equation results, and markers denote stochastic simulations.

In deriving rate equations from the stochastic model, or from more extensive master equations,[2] it is assumed that $\langle n_p n_e\rangle\simeq\langle n_p\rangle\langle n_e\rangle$. However, this mean-field approximation need not be fulfilled for β-values approaching unity since $1/\beta$ plays the role of a saturation photon number and fluctuations on the scale of just one photon may thus cause saturation of the carrier number.[2] Figure 4 illustrates this point by plotting the simulated ratio $\langle n_p n_e\rangle/\langle n_p\rangle\langle n_e\rangle$ versus pump rate. The dashed line is for the rate equation case, where the mean field approximation is assumed to be valid. Black markers are for the case of $\beta=1$ in Fig. 3 with $n_0=20$, and it is seen that the deviations between stochastic simulations and rate equations occur in the pump range where the mean-field approximation is broken. Figure 4 illustrates that the agreement between the two approaches is not as good for the carrier number as for the photon number, which is again an indication of the importance of carrier number fluctuations in the cavity-QED limit of near-unity β-values.[2] As the number of emitters is further lowered, requiring the laser cavity Q-factor to be increased in order to enable lasing, one finds that the mean-field approximation worsens at low pump powers.

Finally, in Fig. 5, β, γ_t, and γ_c are kept constant, while the number of emitters is varied. For the case of 10 emitters

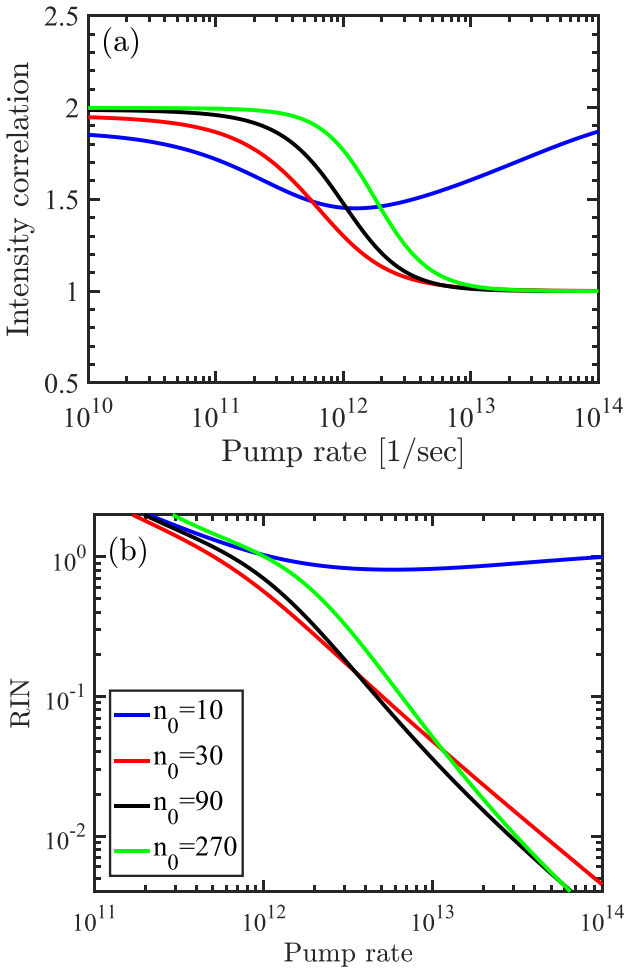

FIG. 5. Dependence on the number of emitters for otherwise fixed parameters. (a) Intensity correlation, $g^{(2)}(0)$, and (b) RIN versus absolute pump rate. The numbers of emitters are $n_0=10$ (blue), 30 (red), 90 (black), and 270 (green), and the fixed parameters are $\beta=0.9$, $\gamma_t=1\times10^{10}\,\mathrm{s}^{-1}$, and $\gamma_c\times10^{11}\,\mathrm{s}^{-1}$.

(blue curve), the laser remains below threshold for all pump powers and a transition to lasing, signified by $g^{(2)}(0) = 1$, is not observed. Peculiarly, a dip is observed in $g^{(2)}(0)$ at intermediate pump rates, which appears to be in good qualitative agreement with experimental results presented in Ref. 10. Due to the fact that threshold, in this case, is not reached even if all the emitters are inverted, i.e., $n_0\gamma_r < \gamma_c$, the output power saturates even in the strong pump limit and the RIN accordingly plateaus at a high level. Notice that in order to observe this behaviour, it is essential to include only a finite number of emitters in the model, ensured by the pump-blocking mechanism in Eqs. (3) and (4). In practice, other transitions may also become important for high pump rates,[39] e.g. multi-excitons in the case of quantum dots, where transitions can also involve the wetting layer.[25]

Even when the number of available emitters, n_0, is large enough to sustain lasing, the threshold pump power depends on the actual emitter number. Thus, achieving the transparency condition of zero material gain requires inverting, on average, half of the emitters, cf. Eq. (6). This means that the noise performance is optimum at a specific number of emitters and then degrades when adding more emitters to the laser cavity. For large output power, when the lasers all are pumped highly above threshold, the performance of the lasers becomes very similar.

In conclusion, we analyzed a rate equation model valid for nanolasers with discrete emitters. We considered the good-cavity limit, valid for most semiconductor lasers, where the emitter broadening is larger than the cavity linewidth. Several conclusions are drawn: (1) The quantum noise properties, including the second-order intensity correlation, $g^{(2)}(0)$, are well accounted for by analytical expressions, derived using the Langevin approach, in the entire region from below to above threshold, at least for more than 10 emitters; (2) The noise properties are improved by increasing the spontaneous emission β-factor; (3) Purcell enhancement effects are already included in standard semiconductor laser rate equations when excluding the bad-cavity limit; and (4) for a given laser cavity, there is an optimum number of emitters.

One of the authors (J.M.) acknowledges helpful discussions with Igor Protsenko, Niels Gregersen, and Andrea Fiore, as well as financial support from Villum Fonden via the NATEC Centre (Grant No. 8692).

[1]G. Bjork and Y. Yamamoto, IEEE J. Quantum Electron. **27**, 2386 (1991).
[2]P. R. Rice and H. J. Carmichael, Phys. Rev. A-At. Mol. Opt. Phys. **50**, 4318 (1994).
[3]T. Wang, G. P. Puccioni, and G. L. Lippi, Sci. Rep. **5**, 15858 (2015).
[4]L. A. Coldren, S. W. Corzine, and M. L. Masanovic, *Optical Engineering*, 2nd ed. (Wiley, 2012).
[5]S. Noda, Science **314**(80), 260 (2006).
[6]I. Prieto, J. M. Llorens, L. E. Muñoz-Camúñez, A. G. Taboada, J. Canet-Ferrer, J. M. Ripalda, C. Robles, G. Muñoz-Matutano, J. P. Martínez-Pastor, and P. A. Postigo, Optica **2**, 66 (2015).
[7]M. Takiguchi, H. Taniyama, H. Sumikura, M. D. Birowosuto, E. Kuramochi, A. Shinya, T. Sato, K. Takeda, S. Matsuo, and M. Notomi, Opt. Express **24**, 3441 (2016).
[8]Y. Ota, M. Kakuda, K. Watanabe, S. Iwamoto, and Y. Arakawa, Opt. Express **25**, 19981 (2017).
[9]M. Lermer, N. Gregersen, M. Lorke, E. Schild, P. Gold, J. Mork, C. Schneider, A. Forchel, S. Reitzenstein, S. Höfling, and M. Kamp, Appl. Phys. Lett. **102**, 052114 (2013).
[10]S. Kreinberg, W. W. Chow, J. Wolters, C. Schneider, C. Gies, F. Jahnke, S. Höfling, M. Kamp, and S. Reitzenstein, Light Sci. Appl. **6**, e17030 (2017).
[11]M. Khajavikhan, A. Simic, M. Katz, J. H. Lee, B. Slutsky, A. Mizrahi, V. Lomakin, and Y. Fainman, Nature **482**, 204 (2012).
[12]H. Yokoyama and S. D. Brorson, J. Appl. Phys. **66**, 4801 (1989).
[13]E. K. Lau, A. Lakhani, R. S. Tucker, and M. C. Wu, Opt. Express **17**, 7790 (2009).
[14]T. Suhr, N. Gregersen, K. Yvind, and J. Mork, Opt. Express **18**, 11230 (2010).
[15]N. Gregersen, T. Suhr, M. Lorke, and J. Mork, Appl. Phys. Lett. **100**, 131107 (2012).
[16]A. Moelbjerg, P. Kaer, M. Lorke, B. Tromborg, and J. Mørk, IEEE J. Quantum Electron. **49**, 945 (2013).
[17]A. Lebreton, I. Abram, N. Takemura, M. Kuwata-Gonokami, I. Robert-Philip, and A. Beveratos, New J. Phys. **15**, 033039 (2013).
[18]K. Ding, J. O. Diaz, D. Bimberg, and C. Z. Ning, Laser Photonics Rev. **9**, 488 (2015).
[19]W. Cartar, J. Mørk, and S. Hughes, Phys. Rev. A **96**, 023859 (2017).
[20]B. Romeira and A. Fiore, IEEE J. Quantum Electron. **54**, 1–12 (2018).
[21]H. E. Türeci, A. D. Stone, and B. Collier, Phys. Rev. A **74**, 043822 (2006).
[22]P. T. Kristensen and S. Hughes, ACS Photonics **1**, 2 (2014).
[23]K. Ujihara, Opt. Commun. **103**, 265 (1993).
[24]P. Kaer, T. R. Nielsen, P. Lodahl, A.-P. Jauho, and J. Mork, Phys. Rev. B **86**, 085302 (2012).
[25]M. Settnes, P. Kaer, A. Moelbjerg, and J. Mork, Phys. Rev. Lett. **111**, 067403 (2013).
[26]E. Purcell, Proc. Am. Phys. Soc. **69**, 681 (1946).
[27]J.-M. Gerard, *Single Quantum Dots* (Springer, 2003), pp. 269–315.
[28]M. P. van Exter, S. J. M. Kuppens, and J. P. Woerdman, Phys. Rev. A **51**, 809 (1995).
[29]I. Protsenko, E. C. André, A. Uskov, J. Mørk, and M. Wubs, preprint arXiv:1709.08200 (2017).
[30]S. Matsuo, T. Sato, K. Takeda, A. Shinya, K. Nozaki, H. Taniyama, M. Notomi, K. Hasebe, and T. Kakitsuka, IEEE J. Sel. Top. Quantum Electron. **19**, 4900311 (2013).
[31]W. Xue, Y. Yu, L. Ottaviano, Y. Chen, E. Semenova, K. Yvind, and J. Mork, Phys. Rev. Lett. **116**, 063901 (2016).
[32]J. P. Dowling, M. Scalora, M. J. Bloemer, and C. M. Bowden, J. Appl. Phys. **75**, 1896 (1994).
[33]S. Ek, P. Lunnemann, Y. Chen, E. Semenova, K. Yvind, and J. Mork, Nat. Commun. **5**, 5039 (2014).
[34]J. Mørk and T. R. Nielsen, Opt. Lett. **35**, 2834 (2010).
[35]N. van Druten, Y. Lien, C. Serrat, S. Oemrawsingh, M. van Exter, and J. Woerdman, Phys. Rev. A **62**, 053808 (2000).
[36]G. P. Puccioni and G. L. Lippi, Opt. Express **23**, 2369 (2015).
[37]W. W. Chow, F. Jahnke, and C. Gies, Light Sci. Appl. **3**, e201 (2014).
[38]F. Jahnke, C. Gies, M. Aßmann, M. Bayer, H. A. M. Leymann, A. Foerster, J. Wiersig, C. Schneider, M. Kamp, and S. Höfling, Nat. Commun. **7**, 11540 (2016).
[39]S. Ritter, P. Gartner, C. Gies, and F. Jahnke, Opt. Express **18**, 9909 (2010).